

The micromagnetic modeling and simulation kit M³S for the simulation of the dynamic response of ferromagnets to electric currents

Massoud Najafi ^{a,b*}, Benjamin Krüger ^c, Stellan Bohlens ^c, Gunnar Selke ^a,
Bernd Güde ^{a,b}, Markus Bolte ^{a,b}, and Dietmar P. F. Möller ^a

*mailto://mnajafi@physnet.uni-hamburg.de,

^a Arbeitsbereich Technische Informatik Systeme, Department Informatik, Universität Hamburg, Vogt-Kölln-Straße 30, 22527 Hamburg, Germany,

^b Institut für Angewandte Physik und Zentrum für Mikrostrukturforschung, Universität Hamburg, Jungiusstraße 11, 20355 Hamburg, Germany,

^c I. Institut für Theoretische Physik, Universität Hamburg, Jungiusstraße. 9, 20355 Hamburg, Germany

Keywords: simulation of physical phenomena, micromagnetic modelling and simulation, spin valves, spin-transfer torque

Abstract

Micro- and nanostructured ferromagnetic materials are actively studied as they offer a variety of applications for microelectronics, hard disks and main memory devices. The widely accepted standard model to describe ferromagnetic systems in this regime is the micromagnetic model [1]. Recently, the interaction of electric currents with the local magnetization in a ferromagnet by transfer of spin momentum have become a focus in academic and industrial research. Hence it has become necessary to extend the micromagnetic model by current-dependent terms, known as the spin-transfer torque extensions. This work presents the micromagnetic modeling and simulation kit M³S, which implements the basic micromagnetic model as well as the spin-transfer torque extensions for multilayer systems based on Slonczewski [2, 3] and the spin-transfer torque extension for continuously varying magnetization based on Zhang and Li [4]. The architecture of the M³S is discussed and the validity of the implementation is proven by several test problems.

1. INTRODUCTION

The micromagnetic model [1] describes the magnetization dynamics by a time-dependent non-linear partial differential equation, the so-called Landau-Lifshitz-Gilbert equation (LLG) and includes the spatial interaction by different magnetic field terms [5]. In the beginning the micromagnetic model was used for analytical calculations of the widths of magnetic domain walls or the switching field in very small ferromagnetic particles. In recent years, through the rise of powerful computers, micromagnetic modeling and simulation have evolved into an important method for investigations in this field of research, because they enable the prediction and interpretation of the dynamic behavior of existing and virtual ferromagnetic systems. They also constitute

a major factor in gaining a deeper understanding of the fundamental physical principles. Even more recently, the interaction of electric currents with the local magnetization in a ferromagnet have become a focus in this field of research. One example is discovery of the giant magnetoresistance effect [6, 7] for which P. Grünberg and A. Fert were awarded the Nobel Prize. New physical phenomena were integrated into the micromagnetic model by adding current-dependent torque terms, known as the spin-transfer torque terms, into the LLG equation [2, 4, 8]. Nowadays, two different current-dependent extensions of the LLG equation exist: The first, developed by Slonczewski [2], accurately describes currents traversing through interfaces between ferromagnets and non-magnets and the ensuing torque on the magnetization. The second was developed by Berger [8] and has since been extended by Zhang and Li [4] and Thiaville et al. [9]. It deals with the spin-transfer torque due to continuous changes in the magnetization, e.g., due to domain walls or magnetic vortices.

This work will present the micromagnetic modeling and simulation kit M³S as an advancement of a micromagnetic simulation tool prototype presented at the Summer Computer Simulation Conference (SCSC) in San Diego in 2007[10]. It implements both versions of the spin-transfer torque term. The outline of this work is as follows: Section 2 describes the micromagnetic model and both spin-transfer torque extensions. Section 3 then presents M³S with the spin-transfer torque module and discuss the benefits of its architecture. Section 4 validates M³S by comparing the results of well defined structures with analytical and experimental results.

2. THEORETICAL BACKGROUND

In this section the micromagnetic model, which is the appropriate model to describe ferromagnets on the nano- and micrometer scale, as well as the spin-transfer torque extensions are described in more detail.

2.1. Micromagnetic Model

The micromagnetic model correctly predicts the static structure of nano- and micrometer-sized ferromagnets as well as the dynamics up to the THz-regime. In 1932, Landau and Lifshitz [5] laid the foundation to this theory, with major contributions coming later from Gilbert, Néel, Bloch, Brown, and many others [1, 11, 12]. Several excellent reviews and books describe this theory in great detail [13, 14, 15]. In this model the ferromagnet's magnetization wants to align itself to the magnetic fields that are present in each point of the volume. In turn the magnetization determines the effective magnetic field by a superposition of internal and external magnetic fields. The internal fields are caused by different magnetic interactions such as the quantummechanical exchange between neighboring spins or the magnetostatic interaction. The interaction between magnetization and effective field leads to a complex dynamic behavior. Except for some analytically feasible systems, the magnetization dynamics can only be solved numerically.

2.1.1. Equation of Motion

The LLG equation is the fundamental equation in the micromagnetic model and describes the motion of the magnetization. The magnetization \vec{M} precesses around the local effective magnetic field \vec{H}_{eff} and is damped towards its equilibrium direction, which is parallel to the effective field as shown in Fig. 1. It is described by the two terms on the right-hand side of Eqn. (1):

$$\frac{d\vec{M}}{dt} = -\gamma\vec{M} \times \vec{H}_{\text{eff}} + \frac{\alpha}{M_s}\vec{M} \times \frac{d\vec{M}}{dt}, \quad (1)$$

Here M_s is the saturation magnetization, $\gamma = 2.21 \cdot 10^5$ m/C is the absolute value of the gyromagnetic ratio, and $\alpha > 0$ is the Gilbert damping constant.

2.1.2. Effective Field

The micromagnetic model includes all magnetic interactions as magnetic fields interacting with the local magnetic moments. The basic model includes the magnetostatic field, the exchange field, the anisotropy field, and the Zeeman field.

The magnetostatic field describes the magnetic interactions of the local magnetic moments over long distances within the body and favors the magnetization to be aligned to the surface. A magnetization perpendicular to a surface would lead to surface charges akin to electrical charges in a capacity and thus greatly increase the system's energy. The exchange field describes the interaction between the spins of neighboring atoms. In ferromagnets, the exchange interaction tends to align neighbor spins parallel to each other. The interplay between the exchange and magnetostatic interaction leads to the

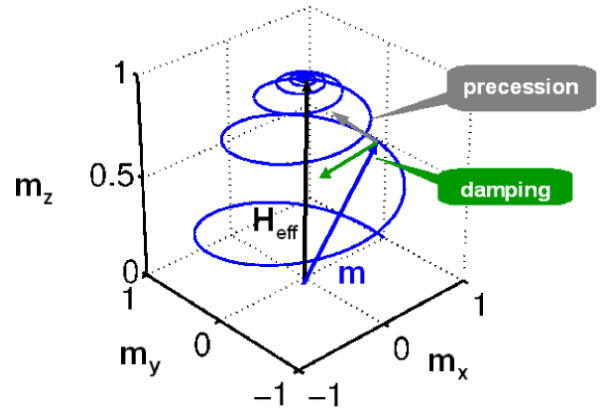


Figure 1. Trajectory of the magnetization due to an effective field. The magnetization performs a damped precession around the effective field.

formation of magnetic domains in the ferromagnet. A domain is a region within the ferromagnet in which the magnetization is fully aligned. The boundaries of two domains in which the magnetization rotates from the direction in one domain to the direction in the other domain are called domain walls. The anisotropy field describes anisotropic effects that arise due to the structure of the lattice and to the particular symmetries that are present in certain crystals. It leads the ferromagnet to magnetize along specific directions, which in literature are referred to as easy axes. The Zeeman field is the field from an external magnet. The local summation of all these field types constitute the local effective field.

2.2. Spin-transfer Torque for Media with Continuously Varying Magnetization

In addition to the standard micromagnetic model, an extension for the interaction of itinerant, i.e., moving electrons and the local magnetization in volumes with continuously changing magnetization have been introduced[4, 8]. It correctly describes magnetization dynamics within a ferromagnet with continuously varying magnetization as shown in Fig. 2, that is excited by a spin-polarized current. The additional torque, called *spin-transfer torque* for such a system arises from the interaction of the spin-polarized current with the local magnetic moments within the ferromagnet. The itinerant electrons align their spin with the spins of the local electrons that constitute the magnetization. This torque on the moving electrons must be compensated by an opposite torque on the local magnetization to conserve the total momentum. The extended LLG with two extra spin-transfer torque terms is[4, 16, 17]

$$\begin{aligned}
\frac{d\vec{M}}{dt} = & -\gamma\vec{M} \times \vec{H}_{\text{eff}} + \frac{\alpha}{M_s}\vec{M} \times \frac{d\vec{M}}{dt} \\
& - \frac{b_j}{M_s^2}\vec{M} \times (\vec{M} \times (\vec{j} \cdot \vec{\nabla})\vec{M}) \\
& - \xi \frac{b_j}{M_s}\vec{M} \times (\vec{j} \cdot \vec{\nabla})\vec{M},
\end{aligned} \quad (2)$$

with the coupling constant $b_j = (P\mu_B)/(eM_s(1 + \xi^2))$ between the current \vec{j} and the magnetization \vec{M} , where μ_B is the Bohr magneton, e is the elementary charge, $\xi = \tau_{\text{ex}}/\tau_{\text{sf}}$ is the degree of non-adiabacity, and P denotes the spin polarization of the current. Equation (2) can be written in explicit form

$$\begin{aligned}
\frac{d\vec{M}}{dt} = & -\gamma'\vec{M} \times \vec{H}_{\text{eff}} - \frac{\alpha\gamma'}{M_s}\vec{M} \times (\vec{M} \times \vec{H}_{\text{eff}}) \\
& - \frac{b'_j}{M_s^2}(1 + \alpha\xi)\vec{M} \times (\vec{M} \times (\vec{j} \cdot \vec{\nabla})\vec{M}) \\
& - \frac{b'_j}{M_s}(\xi - \alpha)\vec{M} \times (\vec{j} \cdot \vec{\nabla})\vec{M},
\end{aligned} \quad (3)$$

with the abbreviations $\gamma' = \gamma/(1 + \alpha^2)$ and $b'_j = b_j/(1 + \alpha^2)$ as shown by Krüger et al.[18].

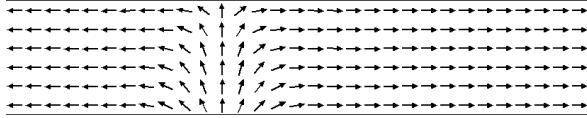


Figure 2. An example for a system with continuous varying magnetization that exhibit the spin-transfer torque effect. In the magnetic wire the magnetization changes continuously from the left to the right. The current flows along the wire direction and interacts with the spatially variation of the magnetization which leads to a motion and distortion of the domain wall.

2.3. Spin-transfer Torque in a Spin Valve

In magnetic multilayers the magnetization changes abruptly at the interfaces between the magnetic layers. The approximation made in the spin-transfer torque model for continuous media cannot be applied for these geometries. In the following section, the spin-transfer torque extension for the description of a spin valve with currents flowing perpendicular-to-plane (CPP) is introduced. A spin valve is a multilayer system, consisting of basically two ferromagnetic layers that are connected by a nonmagnetic metallic spacer as shown in Fig. 3.

In contrast to continuously varying magnetization, the spin-transfer torque in such a spin valve originates from the

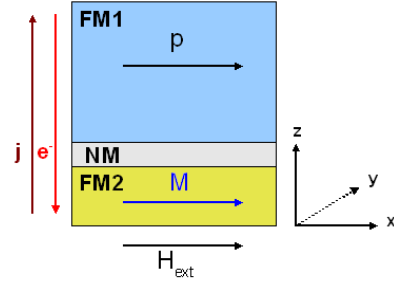


Figure 3. Simple sketch of a spin valve. The electrons flows in $-z$ -direction and crosses first the fixed ferromagnetic layer FM1. FM1 polarizes the current in the direction of his magnetization \vec{p} . The spin-polarized current influences the second ferromagnetic layer FM2 via the spin-transfer torque

interaction of the spin-polarized current with the local magnetic moments at the interface between the ferromagnets and the spacer. The ferromagnetic layer FM1, called the fixed layer, is designed to be unaffected by the spin-transfer torque. In reality, this is achieved by exchange-coupling of FM1 to additional layers, e.g., antiferromagnets. FM1 then serves as a source for the spin-polarized current. All electrons passing through this layer becomes polarized equal to its magnetization direction \vec{p} . The dynamics of the other ferromagnetic layer, called free layer FM2, due to the spin-transfer torque is given by [2, 3, 17, 19]

$$\frac{d\vec{M}}{dt} = -\gamma\vec{M} \times \vec{H}_{\text{eff}} - \frac{\gamma a_j}{M_s}\vec{M} \times (\vec{M} \times \vec{p}) + \frac{\alpha}{M_s}\vec{M} \times \frac{d\vec{M}}{dt}. \quad (4)$$

Here $a_j = M_s\beta g(\theta)$ is the coupling constant between the current and the magnetization, with the angle θ between \vec{M} and \vec{p} , $\beta = \hbar j/(\mu_0 M_s d e)$ and $g(\theta) = \Lambda P/[2((\Lambda^2 + 1) + (\Lambda^2 - 1)\cos\theta)]$. In these equations \hbar is Planck's constant, μ_0 is the permeability of the vacuum, $\Lambda = G \cdot R$, the product of conductance and resistance, differs from unity if the layers have different thicknesses, P is the spin polarization of the current, and d is the thickness of the free layer, [3, 19, 20]. Employing the same abbreviations as in 2.3., equation (4) can be written in its explicit form

$$\begin{aligned}
\frac{d\vec{M}}{dt} = & -\gamma\vec{M} \times \vec{H}_{\text{eff}} - \frac{\gamma\alpha}{M_s}\vec{M} \times (\vec{M} \times \vec{H}_{\text{eff}}) \\
& - \frac{\gamma a_j}{M_s}\vec{M} \times (\vec{M} \times \vec{p}) + \gamma\alpha a_j \vec{M} \times \vec{p}.
\end{aligned} \quad (5)$$

3. M³S

M³S is a framework for the simulation of micromagnetic problems. It is the advanced version of the prototype of

the micromagnetic simulation tool presented at the Summer Computer Simulation Conference (SCSC) in San Diego in 2007[10]. From the developer’s point of view, the purpose of the development of M³S is to create a micromagnetic simulator with a high software quality [21], with a focus on the key attributes high modularity, easy testability, simple extensibility, and high efficiency. Since high modularity and high efficiency are in many cases opposing attributes, every development process must weigh up the possible solutions with respect to these attributes. The easy testability and simple extensibility directly correspond to modularity, because tests need the possibility to check components with manageable complexity. The actual way to deal with this decision is to follow the three steps in the advice of Kent Beck to *Make It Work, Make It Right, Make It Fast*[22].

In addition to the benefits mentioned in the previous publication [10], MATLAB offers a script language [23], providing a notation similar to the mathematic notation. It also provides simple interfaces to lower-level programming languages such as C, C++, or Fortran. For scientific applications the mathematical notation facilitates the first two steps and allows physicists with a moderate knowledge of MATLAB to quickly write code and to create automated tests for the code. An expert in MATLAB now can implement the third step, without the need to know the physics. This approach has proven invaluable in the development of the present framework for which programmers with backgrounds in computer science and as well as physics could contribute according to their area of expertise.

3.1. Basic Architecture

The core of M³S consists of the configuration object, the solver and the integrator. To start a simulation, a configuration object must be filled with the specific problem definition. The configuration object is at this stage of the simulation responsible for the validation of the user inputs. Then the solver is called passing the configuration to it. If the configuration is consistent, it initializes all needed components, e.g., any included fields or the load-and-store functionality. Next the solver starts the time integration loop by calling the time integrator. The time integrator itself uses the function ”calculate-Model” for the calculation of the time derivative of the magnetization $d\vec{M}(t_i)/dt$ for a time t_i , which is needed to compute the magnetization at the time t_{i+1} via the LLG-equation. Figure 4 shows the main components of M³S as well as the flow chart of a simulation run.

3.2. Spin-transfer Torque Module

As mentioned above, the action of a spin-polarized current on a ferromagnet is still under discussion. The spin-transfer torque for continuously varying magnetization and the spin-transfer torque for a spin valve are currently the accepted

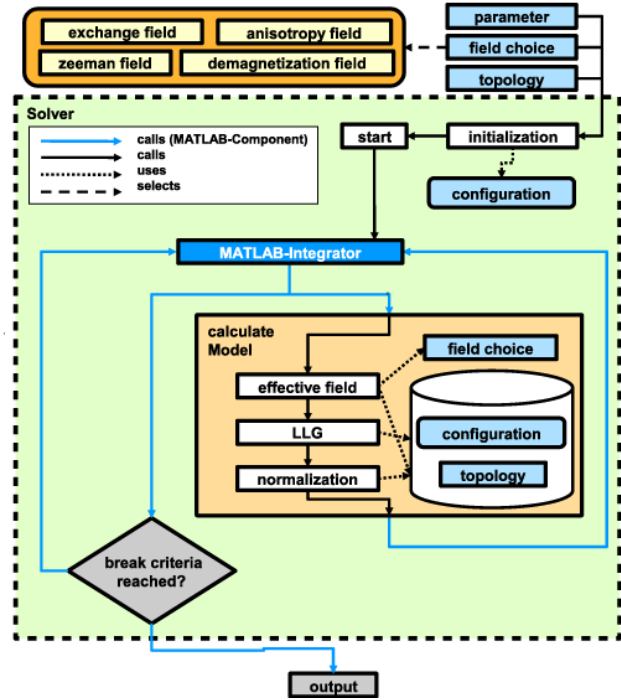


Figure 4. The architecture of M3S showing the interaction of the basic components within a simulation run.

physical descriptions for the respective problem domains. A general description of the spin-transfer torque of continuously and non continuously changing magnetization is still under investigation. Due to these circumstances, it is important to consider the architecture to be flexible for future extensions, without implementing functionality on stock.

The proposed architecture of the module consists of an interface (as shown in Fig.5), which is integrated into the LLG, and the two concrete realizations of spin-transfer torque extensions. To integrate a new spin-transfer torque extension into this architecture, the concrete realization must be implemented. It is important, that it is conformal to the interface. The new extension can then be chosen through the configuration.

4. VALIDATION

Testing the correctness of the simulation results is at least as important as ensuring a good architecture. Therefore, it is important to test individual parts of the simulation, e.g. the field computation or solving the LLG, by unit tests [22] as well as to validate the complete simulation code by integration tests. For the implementation of integration tests the initial parameters and the results of complex micromagnetic reference problems are needed. The μ Mag group[24] has collected such problems, known as standard problems.

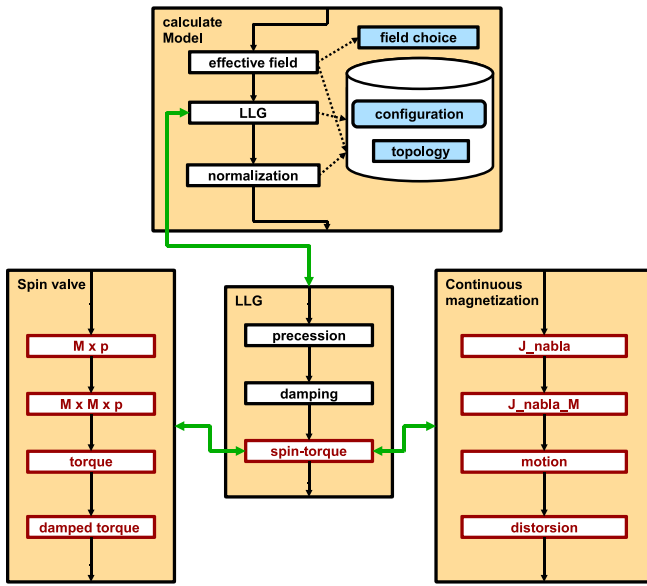


Figure 5. For the simulation, one of the spin-transfer torque extensions can be selected. The selected extension is called from the LLG through a general interface.

The standard problem #4 was used in the previous work to show the correct implementation of the basic micromagnetic model within the prototype [10], which is the basis of M^3S . In order to validate the correctness of M^3S the additional spin-transfer torque modules need to be validated. Since the spin-transfer torque is a new field of research, there are no standard problems, and the model itself is still a matter of active research and discussion. So this work uses approved analytical and computational results as basis of integration tests.

4.1. Spin-transfer Torque for Continuously Varying Magnetization

To confirm the spin-transfer torque module for spin-transfer torque in continuously varying magnetization, the test configuration as shown in Fig. 6 is used. The sample is a ferromagnetic square with a vortex core in the center. The magnetization is excited by a spin-polarized alternating current.

This structure is well suited for the validation, because it has already been investigated in detail [25, 26, 27, 28] and because there exists an analytical description of the magnetization dynamics[25]. The analytical model describes the vortex core dynamics due to a spin-polarized alternating current or an alternating magnetic field. The selected test configuration is a ferromagnetic square with a sample size of $100 \times 100 \times 10 \text{ nm}^3$. For the ferromagnetic material parameters, the values for permalloy were chosen, i.e., an exchange constant $A = 13 \cdot 10^{-12} \text{ J/m}$, a saturation magnetization $M_s = 8 \cdot 10^5 \text{ A/m}$, a damping constant $\alpha = 0.1$, a de-

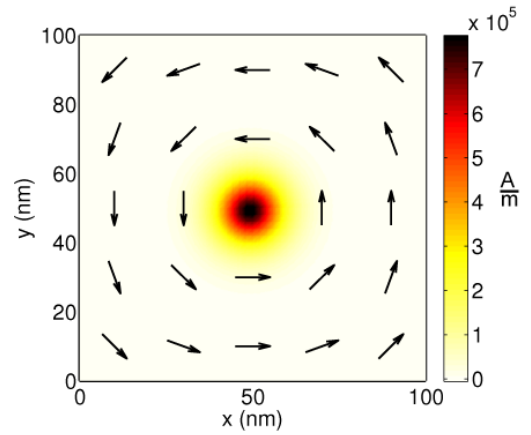


Figure 6. The initial magnetization pattern, a vortex, for the test configuration in this section. The color coding represents the out-of-plane magnetization component.

gree of non-adiabaticity $\xi = 0.05$, and a gyromagnetic ratio $\gamma = 2.211 \cdot 10^5 \text{ m/C}$. The effective field is given by the exchange and magnetostatic field. In addition to the effective field, a spatially homogeneous spin-polarized alternating current of $jP = \cos(\omega t) \cdot 2 \cdot 10^{11} \text{ A/m}^2$ with the frequency of $\omega = 4.4 \text{ GHz}$ is applied in x -direction. The analytical model predicts that the vortex-core excited by such a current starts to gyrate around the center of the ferromagnetic square. Figure 7 shows the results from the simulation with M^3S and the analytical model. As can be seen the resulting trajectory fits excellently to the trajectory of the analytical calculation. This shows the validity of this part of the spin-transfer torque module.

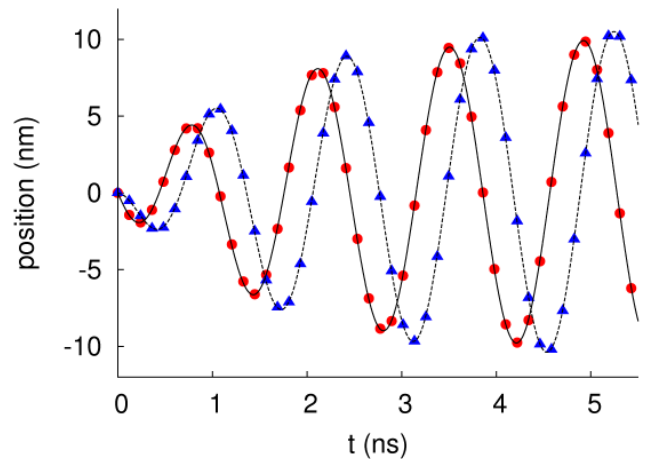


Figure 7. Calculated positions of a vortex that is excited with an alternating current versus simulation time. The circles and triangles denote the x - and y -positions of the vortex, respectively. The lines are fits with the analytical results of Krüger et al. [25].

4.2. Spin-transfer Torque in a Spin Valve

The correctness of the spin-transfer torque module for simulations of the spin-transfer torque in a spin valve is validated by using a rectangular spin valve consisting of two layers of cobalt connected by a copper spacer as a test configuration. This structure was chosen as it has previously been investigated by Li et al. [20] with a edge length $b = 64\text{nm}$ and by Berkov et al. [29] for edge lengths between 16 and 120 nm. As integration test for this module, $b = 20\text{ nm}$ and $b = 48\text{ nm}$ was chosen, because the simulation results for these edge lengths lead to a distinct trajectory of the magnetization. The simulation parameters of the free layer are a saturation magnetization $M_s = 1.2 \cdot 10^7 / (4 \cdot \pi)\text{ A/m}$, a damping constant $\alpha = 0.03$, a spin-transfer torque coupling constant $a_j = -4 \cdot 10^5 / 4 \cdot \pi$ and a gyromagnetic ratio $\gamma = 2.211 \cdot 10^5\text{ m/C}$.

The current flows in negative z -direction through the spin valve. The external field, the easy axis of the crystal anisotropy and the current polarization are aligned in x -direction as shown in Fig. 8. The effective field is given by the exchange field with the exchange constant of $A = 2 \cdot 10^{-11}\text{ J/m}$, the magnetostatic field, the uniaxial anisotropy field with $H_k = 5 \cdot 10^5 / (4 \cdot \pi)\text{ A/m}$, and the uniform Zeeman field with $H_{ext} = 1.75 \cdot 10^6 / (4 \cdot \pi)\text{ A/m}$.

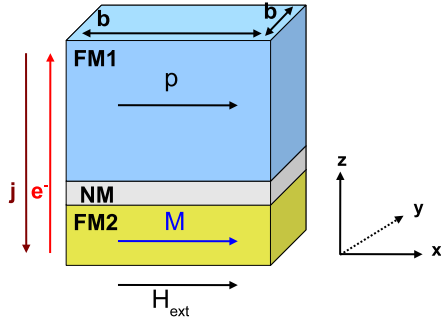


Figure 8. Scheme of the test system, which was used for the validation of the spin-transfer torque. For the validation this system was investigated with different edge lengths b .

At the beginning of the simulation the magnetization is aligned in y -direction. All simulations were computed according to the parameters given by Berkov et al. [29] with a cell size of $2 \times 2 \times 2.5\text{ nm}^3$ in (x,y,z) -direction. Figure 9 shows the results for $b = 20\text{ nm}$. The time resolved magnetization component m_x as well as the trajectory of the magnetization match well with the results of Berkov et al. Figure 10 shows the results for $b = 48\text{ nm}$. The results of this problem differ in the time resolved magnetization component, but the trajectory of the magnetization match well with the results of Berkov et al. Since in their publication the magnetostatic field causes the difference between $b = 20\text{ nm}$ and $b = 48\text{ nm}$, this error can be explained by the difference in the computation

of the magnetostatic field by Berkov et al. In comparison to the results of standard problem #4, this difference has a magnitude of about 2%. We conclude that the spin-transfer torque modules are also valid for the simulation of spin valve systems.

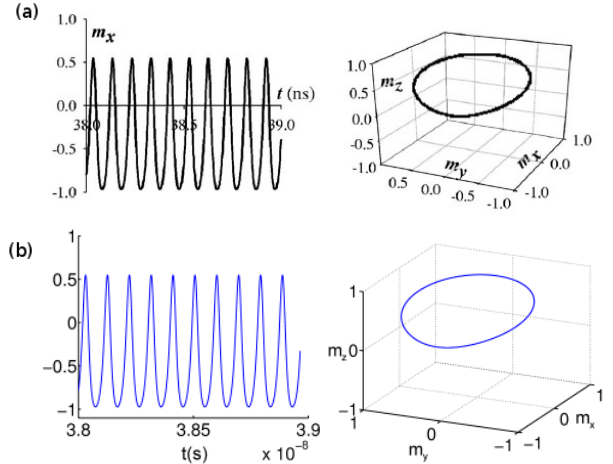


Figure 9. The simulation results for $b = 20\text{ nm}$. a.) shows the results from Berkov et al.[29], b.) shows the results of this work.

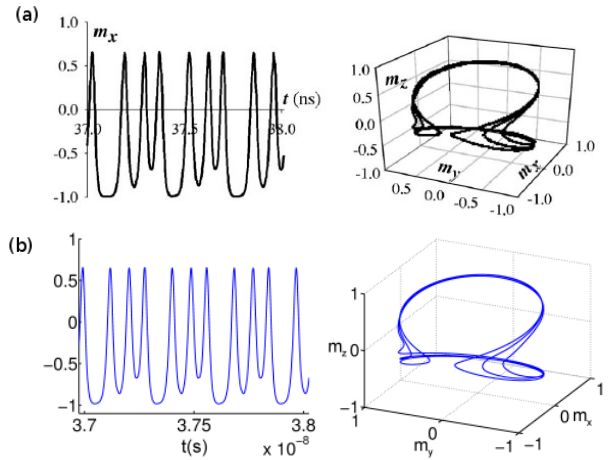


Figure 10. The simulation results for $b = 48\text{ nm}$. a.) shows the results from Berkov et al. [29], b.) shows the results of this work.

5. SUMMARY AND OUTLOOK

We have presented the new micromagnetic modelling and simulation kit M^3S with the spin-transfer torque module. The correctness of the implemented physics was proved by integration tests based on significant problem definitions. The main goal of this implementation is to ensure a high software quality and so to simplify future extensions. Future tasks will be

the expansion of our tool in view of multi threading and parallelization using the Message Passing Interface (MPI). This is necessary to achieve reasonable computation time for tasks such as the simulation of whole ferromagnetic wire or an array of ferromagnetic nano-particles.

6. ACKNOWLEDGMENTS

Financial support by the Deutsche Forschungsgemeinschaft via SFB 668 "Magnetismus vom Einzelatom zur Nanostruktur" and via Graduiertenkolleg 1286 "Functional metal-semiconductor hybrid systems" is gratefully acknowledged.

REFERENCES

- [1] W. F. Brown Jr. *Micromagnetics*. Interscience Publishers, New York, NY, 1963.
- [2] J.C. Slonczewski. Current-driven excitation of magnetic multilayers. *J. Mag. Mag. Mat.*, 159:1–7, 1996.
- [3] J.C. Slonczewski. Currents and torques in metallic magnetic multilayers. *J. Mag. Mag. Mat.*, 247:324–338, 2002.
- [4] S. Zhang and Z. Li. Roles of nonequilibrium conduction electrons on the magnetization dynamics of ferromagnets. *Phys. Rev. Lett.*, 93:127204, 2004.
- [5] L. Landau and E. Lifshitz. On the theory of the dispersion of magnetic permeability in ferromagnetic bodies. *Physik. Z. Sowjetunion*, 8:153–169, 1935.
- [6] M. N. Baibich, A. Fert Broto, J. M., and F. Nguyen Van Dau. Giant magnetoresistance of (001)fe/(001)cr magnetic superlattices. *Phys. Rev. Lett.*, 61:2472–2475, 1988.
- [7] G. Binasch, P. Grünberg, F. Saurenbach, and W. Zinn. Enhanced magnetoresistance in layered magnetic structures with antiferromagnetic interlayer exchange. *Phys. Rev. B*, 39:4828–4830, 1989.
- [8] L. Berger. Emission of spin waves by a magnetic multilayer traversed by a current. *Phys. Rev. B*, 54:9353–9358, 1996.
- [9] A. Thiaville, Y. Nakatani, J. Miltat, and Y. Suzuki. Micromagnetic understanding of current-driven domain wall motion in patterned nanowires. *Europhys. Lett.*, 69:990, 2005.
- [10] M.-A. B. W. Bolte and M. Najafi. Simulating magnetic storage elements: Implementation of the micromagnetic model into matlab - case study for standardizing simulation environments, 2007. SCSC 07:Proceedings of the 2007 Summer Computer Simulation Conference, 525.
- [11] F. Bloch. Zur Theorie des Austauschproblems und der Remanenzerscheinung der Ferromagnetika. *Zeitschrift für Physik A Hadrons and Nuclei*, 74:295–335, 1932.
- [12] L. Néel. Some theoretical aspects of rock-magnetism. *C. R. Acad. Sci.*, 241:533, 1955.
- [13] A. Aharoni. *Introduction to the Theory of Ferromagnetism*. Oxford University Press, Oxford, Clarendon, 1963.
- [14] A. Hubert and R. Schäfer. *Magnetic Domains: The Analysis of Magnetic Microstructures*. Springer, Berlin, Germany, 1998.
- [15] H. Kronmüller and M. Fähnle. *Micromagnetism and the Microstructure of Ferromagnetic Solids*. Oxford University Press, Oxford, UK, 1963.
- [16] S. Zhang and Z. Li. Spin-transfer torque for continuously variable magnetization. *Phys. Rev. Lett.*, 73:054428, 2006.
- [17] D.V. Berkov and J. Miltat. Spin-torque driven magnetization dynamics: Micromagnetic modeling. *J. Mag. Mag. Mat.*, 320:1238–1259, 2008.
- [18] B. Krüger, D. Pfannkuche, M. Bolte, G. Meier, and U. Merkt. Current-driven domain-wall dynamics in curved ferromagnetic nanowires. *Phys. Rev. B*, 75:054421, 2007.
- [19] J. Xiao, A. Zangwill, and M. D. Stiles. Boltzmann test of slonczewski's theory of spin-transfer torque. *Phys. Rev. B*, 70:172405, 2004.
- [20] Z. Li and S. Zhang. Magnetization dynamics with a spin-transfer torque. *Phys. Rev. B*, 68:024404, 2003.
- [21] B. W. Boehm, J. R. Brown, and M. Lipow. Quantitative evaluation of software quality. *ICSE '76: Proceedings of the 2nd international conference on Software engineering*, pages 592–605, 1976.
- [22] K. Beck. *Test Driven Development: By Example*. Addison-Wesley, 2003.
- [23] <http://www.mathworks.co.uk/products/matlab/>, 2008.
- [24] <http://www.ctcms.nist.gov/rdm/mumag.org.html>, 2008.
- [25] B. Krüger, A. Drews, M. Bolte, U. Merkt, D. Pfannkuche, and G. Meier. Vortices as harmonic oscillators. *Phys. Rev. B*, 76:224426, 2007.
- [26] V. Novosad, F. Y. Fradin, P. E. Roy, K. S. Buchanan, K. Yu. Guslienko, and S. D. Bader. Magnetic vortex resonance in patterned ferromagnetic dots. *Phys. Rev. B*, 72:024455, 2005.

- [27] A. Drews, B. Krüger, M. Bolte, and G. Meier. Current- and field-driven magnetic antivortices. *Phys. Rev. B*, 77: 094413, 2008.
- [28] M. Bolte, G. Meier, B. Krüger, A. Drews, R. Eiselt, L. Bocklage, S. Bohlens, T. Tyliczszak, A. Vansteenkiste, B. Van Waeyenberge, K. W. Chou, A. Puzic, and H. Stoll. Time-resolved x-ray microscopy of spin-torque-induced magnetic vortex gyration. *Phys. Rev. Lett.*, 100:176601, 2008.
- [29] D. Berkov and N. Gorn. Transition from the macrospin to chaotic behavior by a spin-torque driven magnetization precession of a square nanoelement. *Phys. Rev. B*, 71:052403, 2005.